

# Adsorbed films of three-patch colloids: Continuous and discontinuous transitions between thick and thin films

C. S. Dias,<sup>\*</sup> N. A. M. Araújo,<sup>†</sup> and M. M. Telo da Gama<sup>‡</sup>

*Departamento de Física, Faculdade de Ciências, Universidade de Lisboa, P-1749-016 Lisboa, Portugal and Centro de Física Teórica e Computacional, Universidade de Lisboa, Avenida Professor Gama Pinto 2, P-1649-003 Lisboa, Portugal*

(Received 12 May 2014; published 15 September 2014)

We investigate numerically the role of spatial arrangement of the patches on the irreversible adsorption of patchy colloids on a substrate. We consider spherical three-patch colloids and study the dependence of the kinetics on the opening angle between patches. We show that growth is suppressed below and above minimum and maximum opening angles, revealing two absorbing phase transitions between thick and thin film regimes. While the transition at the minimum angle is continuous, in the directed percolation class, that at the maximum angle is clearly discontinuous. For intermediate values of the opening angle, a rough colloidal network in the Kardar-Parisi-Zhang universality class grows indefinitely. The nature of the transitions was analyzed in detail by considering bond flexibility, defined as the dispersion of the angle between the bond and the center of the patch. For the range of flexibilities considered we always observe two phase transitions. However, the range of opening angles where growth is sustained increases with flexibility. At a tricritical flexibility, the discontinuous transition becomes continuous. The practical implications of our findings and the relation to other nonequilibrium transitions are discussed.

DOI: [10.1103/PhysRevE.90.032302](https://doi.org/10.1103/PhysRevE.90.032302)

PACS number(s): 82.70.Dd, 05.70.Fh, 68.35.Rh

## I. INTRODUCTION

The promise of control, through the colloidal valence, the local arrangements of colloidal networks has posed patchy colloids under the spotlight [1–7]. Due to the highly directional colloid-colloid interaction [8–10] and the possibility of combining different patch types [11–16], the equilibrium phase diagrams are colorful [17–20], yielding a seemingly endless list of new features of practical interest [21–23].

The quest for the feasibility of the equilibrium structures has shifted the emphasis to the kinetics [24–27], in particular to the adsorption on substrates [28–32]. Substrates simultaneously improve the control over assembly [33–37] and provide an identifiable growth direction, which helps to characterize the time evolution of growth and to develop strategies to obtain heterogeneous materials [38]. The ultimate goal is to combine flat or templated substrates and tunable patchy colloids to fashion a new family of metamaterials.

The focus of the theoretical and experimental work has been on the directionality of the interactions with the role of the patch spatial arrangement largely overlooked. However, recent theoretical [39–42] and experimental [43,44] studies have revealed a strong dependence of the equilibrium structures of patchy colloids on the valence and strength of the interactions. Here, as a first step to understand the role of patch-patch correlations on the kinetics of aggregation, we consider the limit of irreversible adsorption with advective mass transport towards the substrate. To access large-length and long-time scales, we choose not to perform detailed molecular dynamics simulations and use, instead, a stochastic model previously proposed in Ref. [30]. As schematically represented in Fig. 1 we consider three-patch spherical colloids and characterize the

patch arrangement by the opening angle  $\delta$  between a reference patch and the other two (adjustable patches). We found a strong dependence of the kinetics on  $\delta$ . In particular, sustained growth of a colloidal network is only possible for a finite range of opening angles  $\delta$ , above  $\delta_{\min}$  and below  $\delta_{\max}$ . We show that the approach to these thresholds can be described as transitions to absorbing states, driven by different mechanisms and of different nature. While the transition at  $\delta_{\min}$  is continuous, that at  $\delta_{\max}$  may be discontinuous.

In the following section we give a description of the model. In Sec. III, we report the results in three sections: Sec. III A, the transition at the minimum opening angle; Sec. III B, the transition at the maximum opening angle; and Sec. III C, the effect of bond flexibility. Finally, in Sec. IV, we draw some conclusions.

## II. MODEL

We consider spherical three-patch colloids of unit diameter  $\sigma$  and a two-dimensional system with a flat substrate at height  $h = 0$ . We also define  $h_{\max}$  as the maximum height of a colloid in the network and assume an initially empty substrate, such that  $h_{\max} = 0$ . To describe the advective transport, we iteratively generate a horizontal position uniformly at random at a height  $h_{\text{dep}} = h_{\max} + \sigma$  and simulate the ballistic downward movement until the colloid either hits the substrate or another colloid. The colloid-substrate collision always results in adsorption of the colloid with a random orientation.

The patch-patch short-range interaction is described in a stochastic way as first proposed in Ref. [30]. We focus on chemical or DNA mediated bonds [8,45], which are highly directional and very strong, and may be considered irreversible within the time scale of interest [46]. Thus, we assume that two patches bond in an irreversible way, a process we name binding, and that bonds are optimal such that the center of two bonded colloids is always aligned with their bonding

<sup>\*</sup>csdias@fc.ul.pt

<sup>†</sup>nmaraujo@fc.ul.pt

<sup>‡</sup>margarid@cii.fc.ul.pt

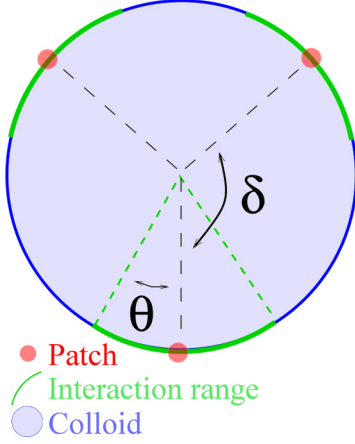


FIG. 1. (Color online) Schematic representation of patches (red) on the surface of a three-patch colloid (blue) and their interaction range  $\theta$  (green). The distribution of patches is described by an opening angle  $\delta$ , in units of  $\pi$  rad, from the center of the two patches and the center of the reference one. The (red) patch is the bonding site and its interaction range (green) represents the extent of the attractive interaction between patches.

patches. We define for each patch an interaction range around the patch, represented by the thick (green) line in Fig. 1, which accounts for both the extension of the patch and the range of the patch-patch interaction. The interaction range is characterized by a single parameter  $\theta = \pi/6$ , representing the maximum angle with the center of the patch (see Fig. 1). Two patches may bind if their interaction ranges partially overlap in the event of a collision. Thus, stochastically, when the incoming colloid hits the interaction range of a colloid in the network, it binds irreversibly to it with a probability  $p = A_{ir}/A$ , where  $A = \pi\sigma$  is the surface of the colloid and  $A_{ir}$  is the extension of the surface covered by the interaction range of all patches. In the case of successful binding, the binding patch of the incoming colloid is chosen uniformly at random among its three patches and its position and orientation is adjusted accordingly. Since the network colloid position and orientation are assumed irreversibly fixed, the alignment of the new binding patches results solely from the rotation and translation of the incoming colloid.

### III. RESULTS

We performed simulations for different opening angles  $\delta$  (in units of  $\pi$  rad) and lengths of the substrate  $L$  (in units of the colloid diameter). For  $\delta < \delta_{\min}$ , the angle between patches is such that all patches are in the same hemisphere. Colloids in the network will most likely have all patches towards the substrate and incoming colloids will fail to bind. Thus, when no more colloids can adsorb on the substrate and after a handful of patch-patch bindings, the growth is suppressed. For  $\delta > \delta_{\max}$ , the two adjustable patches are so close that only one can effectively bind due to the excluded volume interaction, i.e., when one colloid binds to one of the adjustable patches it inevitably shields the access of a new colloid to the second adjustable patch. This also hinders growth due to a more subtle mechanism. Since only one of the adjustable patches can bind,

branching is suppressed and only linear colloidal chains grow out of the substrate. For  $\delta_{\max} < \delta < 1$  these chains are locally tilted and the growth direction fluctuates around the vertical direction. As it fluctuates, the orientation of the patches at the tip will eventually point down and the growth of the chain will be suppressed. Since binding is irreversible and occurs only when an incoming colloid joins the network, the total number of bonds is equal to the number of colloids in the network. The absorbing state occurs when no more patches are available to bind incoming colloids.

For  $\delta_{\min} < \delta < \delta_{\max}$ , a ramified network of patchy colloids grows from the substrate in a sustained fashion. To characterize this growth, we calculate the roughness  $w$  of the interface in the following way. We divide the system in  $N$  vertical slices of width  $\sigma$  ( $N = L/\sigma$ ). For each slice  $i$  we simulate the downward trajectory of a probe colloid released from the center of the slice at  $h_{\text{dep}}$  and calculate the height  $h_i$  at which it first touches either one colloid in the network or the substrate. The roughness is then defined as

$$w = \sqrt{\frac{1}{N} \sum_i [h_i - \bar{h}]^2}, \quad (1)$$

where  $\bar{h} = \sum_i h_i/N$ . For all system sizes, the roughness initially increases with the number of colloids and saturates at  $w_{\text{sat}}$ , which depends on  $\delta$  and  $L$ . Figure 2 shows  $w_{\text{sat}}$  as a function of  $\delta$  for different  $L$ . A nonmonotonic dependence on  $\delta$  is observed with a minimum at  $\delta \approx 2/3$ . This minimum occurs when the three patches are equidistant, which favors branching and consequently leads to a decrease of the roughness. Snapshots of the colloidal network for different regimes can be seen in Fig. 3. When  $w_{\text{sat}}$  is rescaled by  $L^{\alpha_{\text{KPZ}}}$ , where  $\alpha_{\text{KPZ}} = 1/2$  is the roughness exponent for the Kardar-Parisi-Zhang universality class [47], data collapse is observed, consistent with this universality class. This result is in contrast to previous experimental results for spherical isotropic colloids, where Poisson-like growth is always observed [48]. Our

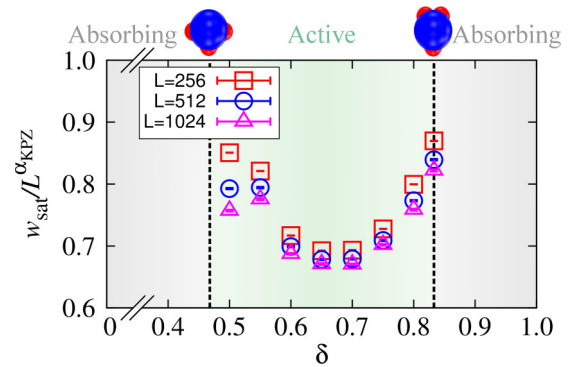


FIG. 2. (Color online) Adsorption of three-patch colloids for different values of the opening angle ( $\delta$ ). Two absorbing phases are found for  $\delta < \delta_{\min}$  and  $\delta > \delta_{\max}$ , where growth is suppressed at a finite thickness. For  $\delta_{\min} < \delta < \delta_{\max}$ , a sustained growth is observed (active phase). The data points are for the data collapse of the roughness in the active phase using  $w_{\text{sat}} = L^{\alpha_{\text{KPZ}}} \mathcal{F}[\delta]$ , where  $\mathcal{F}$  is a scaling function and  $\alpha_{\text{KPZ}}$  is the roughness exponent for the Kardar-Parisi-Zhang universality class. We considered three different lengths of the substrate  $L = \{256, 512, 1024\}$  and results are averages over  $\{320\,000, 80\,000, 40\,000\}$  samples.

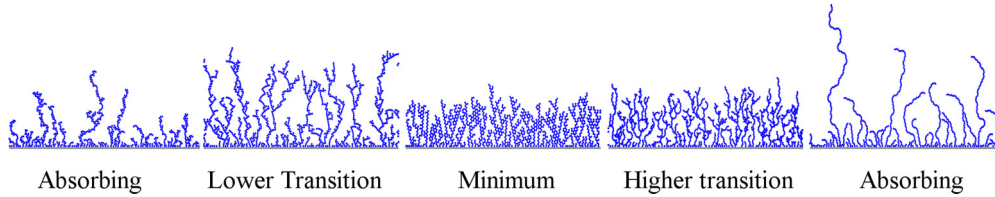


FIG. 3. (Color online) Snapshots for different regimes. From left to right  $\delta = \{0.4, 0.468, 0.666, 0.833, 0.85\}$ . For a system size  $L = 128$  and  $10L$  deposited colloids.

result suggests that the directionality of the interactions leads, always, to a self-affine interface. The behavior for  $\delta \gtrsim \delta_{\min}$  is strongly affected by finite-size effects due to the proximity of the critical point.

We now characterize each transition in detail and estimate the thresholds.

**A. Transition at  $\delta_{\min}$**

As explained before, when all patches are in the same hemisphere the growth is eventually suppressed. Patches of colloids in the network are typically pointing towards the substrate and are thus inaccessible for incoming colloids ballistically approaching the substrate. Considering only the geometrical effect, one expects  $\delta_{\min} = 1/2 - \theta/\pi = 1/3$  (in units of  $\pi$  rad), where the first term refers to the equator and the second to the interaction range.

To estimate the threshold, we performed simulations for different values of  $\delta$ . For each value we ran several samples and attempt the adsorption or binding of  $2048L$  colloids. We considered that growth is suppressed for runs where no attempt is successful after  $64L$  consecutive attempts. Due to strong finite-size effects, as well known for absorbing-phase transitions [49,50], growth is suppressed close to  $\delta_{\min}$  for a fraction of the samples. We have used two different estimators for the threshold. The lower bound ( $\delta_{\min}^{\text{lb}}$ ) is defined as the

highest  $\delta$  for which growth was suppressed in every sample. The upper bound ( $\delta_{\min}^{\text{ub}}$ ) is defined as the lowest  $\delta$  for which growth was never suppressed. Figure 4(a) shows the value of both estimators as a function of  $1/L$ . The linear extrapolation for the thermodynamic limit ( $L \rightarrow \infty$ ) gives  $\delta_{\min}^{\text{lb}} = 0.467 \pm 0.001$  and  $\delta_{\min}^{\text{ub}} = 0.469 \pm 0.002$ . Combining these we obtain  $\delta_{\min} = 0.468 \pm 0.001$ . Due to collective effects during growth, the threshold is higher than that predicted by a purely geometric argument for a single colloid.

A question of practical interest is how fast does the network grow. For stochastic growth models, this can be assessed from the growth rate ( $r$ ), defined as the fraction of successful adsorption/binding attempts [51]. Figure 4(b) shows the dependence of  $r$  on  $\delta$ .  $r$  grows continuously from zero for  $\delta \geq \delta_{\min}$ , meaning that the larger the angle the faster the network grows in mass. To identify the universality class of the absorbing-phase transition at  $\delta_{\min}$  we use  $r$  as the order parameter, which is zero in the absorbing phase and nonzero in the active one. Figure 4(c) depicts the finite-size scaling of the order parameter. A data collapse is obtained over almost three decades with the exponents of the directed percolation (DP) universality class in two dimensions [52–54].

**B. Transition at  $\delta_{\max}$**

The second transition occurs when the distance between the two adjustable patches is such that binding is only possible with one of them. We then expect  $\delta_{\max} = 5/6 \approx 0.83$ , a value that we have confirmed numerically by, as in the continuous case, performing a finite-size study of the transition point (as shown in the inset of Fig. 5). To describe this transition we also use  $r$  as the order parameter. The main plot of Fig. 5 is the histogram of  $r$  for different values of  $\delta$ . While in the absorbing phase ( $\delta > \delta_{\max}$ )  $r = 0$  (not shown), for  $\delta < \delta_{\max}$   $r$  is Gaussianly distributed with a nonzero mean, which converges to  $0.155 \pm 0.001$  at the threshold. In the inset, we show the histogram of  $r$  at  $\delta_{\max}$ , for different system sizes. The larger the system the sharper the distribution. The position of the peak does not show significant size effects, and hence a jump is expected in the thermodynamic limit. Thus, by contrast to the first transition, at  $\delta_{\max}$  the transition is discontinuous and the growth rate jumps at the threshold. Note that, while in the vicinity of  $\delta_{\min}$  the growth rate vanishes with the substrate size, at  $\delta_{\max}$  it does not depend (significantly) on it.

**C. Flexibility**

So far we have considered optimal bonds. This implies that the position of the incoming colloid is adjusted such that the center of the colloids and of their patches is aligned. However,

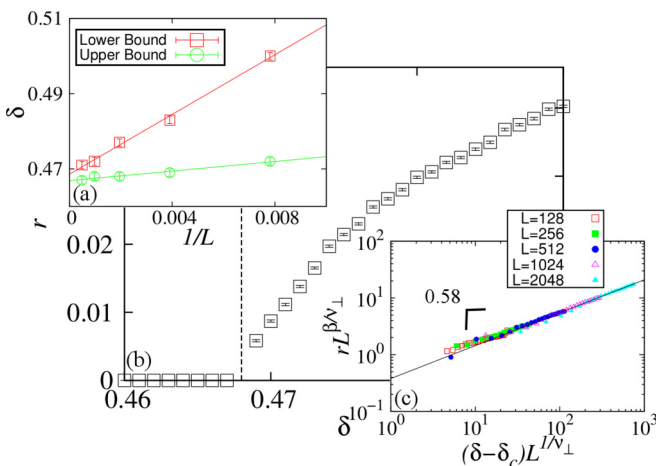


FIG. 4. (Color online) (a) Lower and upper bounds for  $\delta_{\min}$  as a function of  $1/L$ , for  $L = \{128, 256, 512, 1024, 2048\}$  and  $\{1600, 800, 400, 200, 100\}$  samples. (b) Dependence of the growth rate ( $r$ ) on the opening angle ( $\delta$ ) for  $L = 2048$  averaged over  $10^2$  samples. (c) Finite-size scaling for the growth rate, where  $\beta = 0.58$ ,  $\nu_{\perp} = 0.73$ , and  $\delta_c = 0.468$ , consistent with the directed percolation universality class. The system sizes and number of samples are the same as in (a).

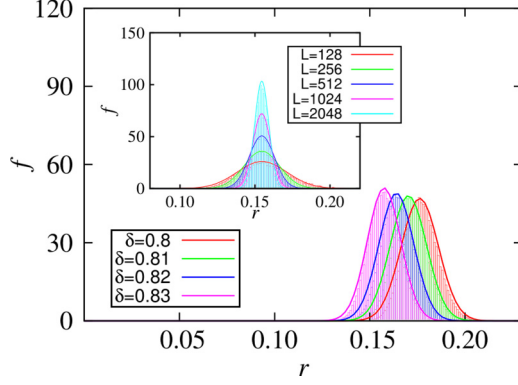


FIG. 5. (Color online) Main plot: Histogram of the growth rate for four values of opening angle close to  $\delta_{\max}$ , namely,  $\delta = \{0.83, 0.82, 0.81, 0.8\}$ , and  $L = 512$ , averaged over  $10^5$  samples. Inset: Histogram of the growth rate at  $\delta_{\max} = \frac{5}{6}$  for  $L = \{128, 256, 512, 1024, 2048\}$ , averaged over  $\{16, 8, 4, 2, 1\} \times 10^5$  samples.

even for chemical bonds, there is some flexibility around the optimal orientation [45,55]. To model nonoptimal bonds we take advantage of the stochastic nature of our model where the relative position and orientation of the colloids after collision may be adjusted. As in the optimal case, since the position and orientation of the network colloid are fixed, only the incoming colloid is adjusted. At a binding event, the flexibility for both rotation and translation of the colloid are represented by an angle  $\gamma$  (see Fig. 6). Inspired by previous models of patchy and DNA-mediated bonds [56,57], the value of  $\gamma$  is drawn randomly from a Gaussian distribution of zero mean and dispersion  $F\theta$ , where  $F$  is the flexibility. Since the patch-patch interaction is short ranged, we truncate the distribution at  $\max\{F\theta, \theta\}$ . The sense of rotation of  $\gamma$  is always from the center of the patch to the point of collision, as illustrated in Fig. 6.

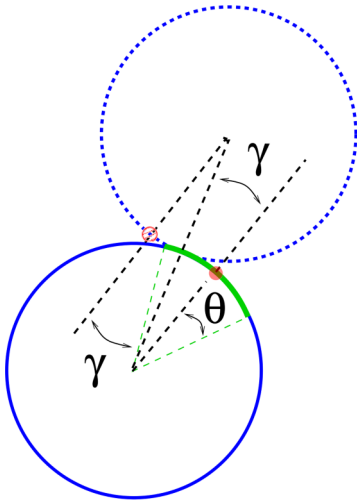


FIG. 6. (Color online) Schematic representation of the flexibility mechanism between bonds: The patch attempting binding will be at a position defined by the angle  $\gamma$  generated by a Gaussian distribution centered at zero, with dispersion  $F\theta$ , truncated at  $F\theta$ . For both colloids, the orientation of the bond is shifted from the ideal one by a randomly generated angle  $\gamma$ .

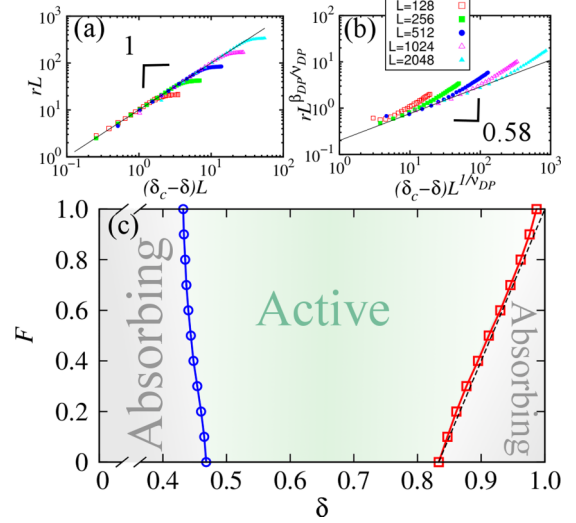


FIG. 7. (Color online) Finite-size scaling for the growth rate rescaled by the exponents of the absorbing transition for (a)  $F = 0.1$  with linear rescaling and (b)  $F = 0.5$  with directed percolation rescaling. Results are for  $L = \{128, 256, 512, 1024, 2048\}$  and averaged over  $\{1600, 800, 400, 200, 100\}$  samples. (c) Phase diagram in the two-parameter space: flexibility ( $F$ ) and opening angle ( $\delta$ ). The (blue-)solid curve in the left-hand side corresponds to the lower threshold ( $\delta_{\min}$ ) and the (red-)solid curve in the right-hand side to the higher one ( $\delta_{\max}$ ). The data points are extrapolations for the thermodynamic limit from the behavior of the size dependence of the thresholds. The (black) dashed curve is the theoretical prediction for  $\delta_{\max}$ .

We performed simulations for different values of  $F$  and  $\delta$ . For the first transition, the value of  $\delta_{\min}$  slightly decreases with  $F$  [see (blue-)solid curve on the left-hand side of Fig. 7(c)]. Yet, for the range of flexibilities considered here the transition is always continuous and in the DP universality class.

For the second transition, the value of  $\delta_{\max}$  increases with  $F$  [(red-)solid curve on the right-hand side of Fig. 7(c)]. Hence, the range of  $\delta$  for which growth is sustained increased with  $F$ . For  $F = 0$  we have shown that the threshold corresponds to the opening angle when two colloids bound to the adjustable patches touch. Likewise, we can estimate the threshold  $\delta_{\max}(F)$  for general  $F$ ,

$$\delta_{\max}(F) = \delta_{\max}(0) + \frac{F\theta}{\pi}, \quad (2)$$

where  $\delta_{\max}(0) = 5/6$  (as discussed before) and the second term corresponds to the maximum value of  $\gamma$ . As shown in Fig. 7(c) [(black-)dashed curve], the threshold values differ by less than 2% from the theoretical prediction. In fact, the difference between the numerical and theoretical values vanishes with decreasing  $F$  and Eq. (2) is exact for  $F = 0$ .

The nature of the transition also changes with the  $F$ . Figures 7(a) and 7(b) depict the data collapses for the order parameter at  $F = 0.1$  and  $F = 0.5$ . At  $F = 0.1$  the transition is still discontinuous and data collapse is obtained with trivial exponents [see Fig. 7(a)]. By contrast, at  $F = 0.5$  the transition is continuous in the DP universality class, as evident from Fig. 7(b). We then expect the nature of the transition to change at a tricritical flexibility (between 0.1 and 0.5), in

the tricritical directed percolation universality class [58,59]. The limit  $F \rightarrow \infty$  corresponds to a uniform distribution of the bonds over the interaction range. In this limit, the active region in the diagram of Fig. 7(c) is maximal.

Figures 7(a) and 7(b) depict two different data collapses, for the order parameter at  $F = 0.1$  and  $F = 0.5$ , with different rescaling of the vertical axis. At  $F = 0.1$  the transition is still discontinuous and data collapse is obtained with linear rescaling typical of a discontinuous transition [see Fig. 7(a)]. By contrast, at  $F = 0.5$  the transition is continuous, and data collapse is obtained by rescaling the vertical axis with the exponents of the DP universality class, as shown in Fig. 7(b).

#### IV. CONCLUSION

We found that the adsorption of patchy colloids on substrates depends strongly on the opening angle between patches. The growth of a colloidal network from the substrate is only sustained between minimum and maximum opening angles. Outside of this active phase the system is trapped into one of two possible absorbing phases where growth is suppressed at a finite thickness of the network. The transitions into the two absorbing phases are quite different. While the transition at the lower threshold is continuous in the DP universality class, that at the higher threshold is discontinuous. We provided an estimator of the higher threshold which is exact in some limits. We also showed that the nature of the transition is intimately related to the growth rate of the network. For a continuous transition the growth rate vanishes in the vicinity of the threshold, while for a discontinuous transition the growth rate has a jump. This difference has obvious practical implications on the feasibility of the predicted structures. We have shown that it is possible to effectively control the interface roughness by varying the opening angle. We are also able to widen the active region of growth by increasing the flexibility of the bonds.

The numerical results were obtained for a two dimensional system but our conclusions may be extended to three

dimensions. However, recent experimental work on colloidal aggregation at the edge of an evaporating drop, may be described as a two-dimensional system [48,60,61]. Such drops may provide a direct experimental realization of our model if patchy colloids with strong bonds are used.

Absorbing phase transitions are the focus of many theoretical [51,52,62,63] and recent experimental works [64–66], including studies that successfully combine both [67,68]. Special attention has been given to nonequilibrium wetting transitions. Also, a change in the nature of the transition is observed at a multicritical strength of the attraction to the substrate. While mesoscopic models predict that the second continuous transition typically falls into the multiplicative noise (MN1) universality class [69,70], they also identify DP transitions [71]. In fact, a crossover from MN1 to DP is expected when varying the control parameter [71]. However, the nonequilibrium wetting phenomenon typically involves three scaling fields; for example, temperature, chemical potential, and surface potential. By contrast, the tricritical transition for patchy colloids presented here is driven by the colloid parameters, namely, the opening angle and flexibility. More importantly, the fluctuations in nonequilibrium wetting models are different from the inherent in our model. Thus, there are interesting possible followups: the identification of the third scaling field, the effect of other fluctuations, and the study of the scaling at the tricritical flexibility. More generally, if desorption and/or bulk thermal fluctuations are included, the transitions between the thin and thick adsorbed films may be related to nonequilibrium wetting phenomena [72,73].

#### ACKNOWLEDGMENTS

We acknowledge financial support from the Portuguese Foundation for Science and Technology (FCT) under Contracts No. EXCL/FIS-NAN/0083/2012, No. PEst-OE/FIS/UI0618/2014, and No. IF/00255/2013.

- 
- [1] A. van Blaaderen, *Nature (London)* **439**, 545 (2006).
  - [2] E. Bianchi, R. Blaak, and C. N. Likos, *Phys. Chem. Chem. Phys.* **13**, 6397 (2011).
  - [3] A. B. Pawar and I. Kretzschmar, *Macromol. Rapid Commun.* **31**, 150 (2010).
  - [4] I. Kretzschmar and J. H. Song, *Curr. Opin. Colloid Interface Sci.* **16**, 84 (2011).
  - [5] M. Grzelczak, J. Vermant, E. M. Furst, and L. M. Liz-Marzán, *ACS Nano* **4**, 3591 (2010).
  - [6] O. I. Wilner and I. Willner, *Chem. Rev.* **112**, 2528 (2012).
  - [7] G.-R. Yi, D. J. Pine, and S. Sacanna, *J. Phys.: Condens. Matter* **25**, 193101 (2013).
  - [8] Y. Wang, D. R. Breed, V. N. Manoharan, L. Feng, A. D. Hollingsworth, M. Weck, and D. J. Pine, *Nature (London)* **491**, 51 (2012).
  - [9] E. Bianchi, J. Largo, P. Tartaglia, E. Zaccarelli, and F. Sciortino, *Phys. Rev. Lett.* **97**, 168301 (2006).
  - [10] J. Russo, P. Tartaglia, and F. Sciortino, *J. Chem. Phys.* **131**, 014504 (2009).
  - [11] J. M. Tavares, P. I. C. Teixeira, and M. M. Telo da Gama, *Mol. Phys.* **107**, 453 (2009).
  - [12] J. M. Tavares, P. I. C. Teixeira, and M. M. Telo da Gama, *Phys. Rev. E* **80**, 021506 (2009).
  - [13] D. de las Heras, J. M. Tavares, and M. M. Telo da Gama, *Soft Matter* **7**, 5615 (2011).
  - [14] J. Hu, S. Zhou, Y. Sun, X. Fang, and L. Wu, *Chem. Soc. Rev.* **41**, 4356 (2012).
  - [15] S. Angioletti-Uberti, B. M. Mognetti, and D. Frenkel, *Nat. Mater.* **11**, 518 (2012).
  - [16] A. Kumar, B. J. Park, F. Tu, and D. Lee, *Soft Matter* **9**, 6604 (2013).
  - [17] J. Russo, J. M. Tavares, P. I. C. Teixeira, M. M. Telo da Gama, and F. Sciortino, *Phys. Rev. Lett.* **106**, 085703 (2011).
  - [18] D. de Las Heras, J. M. Tavares, and M. M. Telo da Gama, *Soft Matter* **8**, 1785 (2012).
  - [19] A. Reinhardt, F. Romano, and J. P. K. Doye, *Phys. Rev. Lett.* **110**, 255503 (2013).
  - [20] F. Smallenburg and F. Sciortino, *Nat. Phys.* **9**, 554 (2013).

- [21] R. Matthews and C. N. Likos, *Phys. Rev. Lett.* **109**, 178302 (2012).
- [22] F. Smalenburg, L. Leibler, and F. Sciortino, *Phys. Rev. Lett.* **111**, 188002 (2013).
- [23] I. Coluzza, P. D. J. van Oostrum, B. Capone, E. Reimhult, and C. Dellago, *Phys. Rev. Lett.* **110**, 075501 (2013).
- [24] F. Sciortino, C. De Michele, S. Corezzi, J. Russo, E. Zaccarelli, and P. Tartaglia, *Soft Matter* **5**, 2571 (2009).
- [25] S. Corezzi, C. De Michele, E. Zaccarelli, P. Tartaglia, and F. Sciortino, *J. Phys. Chem. B* **113**, 1233 (2009).
- [26] S. Corezzi, D. Fioretto, and F. Sciortino, *Soft Matter* **8**, 11207 (2012).
- [27] O. A. Vasilyev, B. A. Klumov, and A. V. Tkachenko, *Phys. Rev. E* **88**, 012302 (2013).
- [28] N. Gnan, D. de Las Heras, J. M. Tavares, M. M. Telo da Gama, and F. Sciortino, *J. Chem. Phys.* **137**, 084704 (2012).
- [29] N. R. Bernardino and M. M. Telo da Gama, *Phys. Rev. Lett.* **109**, 116103 (2012).
- [30] C. S. Dias, N. A. M. Araújo, and M. M. Telo da Gama, *Phys. Rev. E* **87**, 032308 (2013).
- [31] C. S. Dias, N. A. M. Araújo, and M. M. Telo da Gama, *Soft Matter* **9**, 5616 (2013).
- [32] C. S. Dias, N. A. M. Araújo, and M. M. Telo da Gama, *J. Chem. Phys.* **139**, 154903 (2013).
- [33] M. H. S. Shyr, D. P. Wernette, P. Wiltzius, Y. Lu, and P. V. Braun, *J. Am. Chem. Soc.* **130**, 8234 (2008).
- [34] A. B. Pawar and I. Kretzschmar, *Langmuir* **24**, 355 (2008).
- [35] F. Tian, N. Cheng, N. Nouvel, J. Geng, and O. A. Scherman, *Langmuir* **26**, 5323 (2010).
- [36] A. Cadilhe, N. A. M. Araújo, and V. Privman, *J. Phys.: Condens. Matter* **19**, 065124 (2007).
- [37] N. A. M. Araújo, A. Cadilhe, and V. Privman, *Phys. Rev. E* **77**, 031603 (2008).
- [38] T. L. Einstein and T. J. Stasevich, *Science* **327**, 423 (2010).
- [39] G. Doppelbauer, E. Bianchi, and G. Kahl, *J. Phys.: Condens. Matter* **22**, 104105 (2010).
- [40] B. D. Marshall and W. G. Chapman, *J. Chem. Phys.* **139**, 054902 (2013).
- [41] B. D. Marshall and W. G. Chapman, *Phys. Rev. E* **87**, 052307 (2013).
- [42] J. M. Tavares, N. G. Almarza, and M. M. Telo da Gama, *J. Chem. Phys.* **140**, 044905 (2014).
- [43] Y. Iwashita and Y. Kimura, *Soft Matter* **9**, 10694 (2013).
- [44] Y. Iwashita and Y. Kimura, *Soft Matter* **10**, 7170 (2014).
- [45] N. Geerts and E. Eiser, *Soft Matter* **6**, 4647 (2010).
- [46] M. E. Leunissen and D. Frenkel, *J. Chem. Phys.* **134**, 084702 (2011).
- [47] M. Kardar, G. Parisi, and Y.-C. Zhang, *Phys. Rev. Lett.* **56**, 889 (1986).
- [48] P. J. Yunker, M. A. Lohr, T. Still, A. Borodin, D. J. Durian, and A. G. Yodh, *Phys. Rev. Lett.* **110**, 035501 (2013).
- [49] I. Jensen, H. C. Fogedby, and R. Dickman, *Phys. Rev. A* **41**, 3411 (1990).
- [50] A. M. Alencar, J. S. Andrade, Jr., and L. S. Lucena, *Phys. Rev. E* **56**, R2379 (1997).
- [51] F. D. A. Aarão Reis, *Phys. Rev. E* **66**, 027101 (2002).
- [52] M. Henkel, H. Hinrichsen, and S. Lübeck, *Non-equilibrium Phase Transitions* (Springer, Bristol, 2008).
- [53] S. Lübeck, *Int. J. Mod. Phys. B* **18**, 3977 (2004).
- [54] G. Ódor, *Rev. Mod. Phys.* **76**, 663 (2004).
- [55] C. J. Loweth, W. B. Caldwell, X. Peng, A. P. Alivisatos, and P. G. Schultz, *Angew. Chem., Int. Ed.* **38**, 1808 (1999).
- [56] J. Largo, P. Tartaglia, and F. Sciortino, *Phys. Rev. E* **76**, 011402 (2007).
- [57] A. W. Wilber, J. P. K. Doye, A. A. Louis, E. G. Noya, M. A. Miller, and P. Wong, *J. Chem. Phys.* **127**, 085106 (2007).
- [58] S. Lübeck, *J. Stat. Phys.* **123**, 193 (2006).
- [59] P. Grassberger, *J. Stat. Mech.* (2006) P01004.
- [60] P. J. Yunker, D. J. Durian, and A. G. Yodh, *Phys. Today* **66**(8), 60 (2013).
- [61] X. Yang, C. Y. Li, and Y. Sun, *Soft Matter* **10**, 4458 (2014).
- [62] R. M. Ziff, E. Gulari, and Y. Barshad, *Phys. Rev. Lett.* **56**, 2553 (1986).
- [63] J. Marro and R. Dickman, *Nonequilibrium Phase Transitions in Lattice Models* (Cambridge University Press, Cambridge, 1999).
- [64] K. A. Takeuchi, *J. Stat. Mech.* (2014) P01006.
- [65] K. A. Takeuchi, M. Kuroda, H. Chaté, and M. Sano, *Phys. Rev. Lett.* **99**, 234503 (2007).
- [66] L. Shi, M. Avila, and B. Hof, *Phys. Rev. Lett.* **110**, 204502 (2013).
- [67] D. J. Pine, J. P. Gollub, J. F. Brady, and A. M. Leshansky, *Nature (London)* **438**, 997 (2005).
- [68] L. Corté, P. M. Chaikin, J. P. Gollub, and D. J. Pine, *Nat. Phys.* **4**, 420 (2008).
- [69] H. Hinrichsen, R. Livi, D. Mukamel, and A. Politi, *Phys. Rev. E* **61**, R1032 (2000).
- [70] M. A. Muñoz, F. de los Santos, and M. M. Telo da Gama, *Eur. Phys. J. B* **43**, 73 (2005).
- [71] F. Ginelli, V. Ahlers, R. Livi, D. Mukamel, A. Pikovsky, A. Politi, and A. Torcini, *Phys. Rev. E* **68**, 065102(R) (2003).
- [72] F. de los Santos, M. M. Telo da Gama, and M. A. Muñoz, *Europhys. Lett.* **57**, 803 (2002).
- [73] F. de los Santos, M. M. Telo da Gama, and M. A. Muñoz, *Phys. Rev. E* **67**, 021607 (2003).